Dynamics of the formation of an aureole in the bursting of soap films

N. Y. Liang,[1] C. K. Chan,[2,*] and H. J. Choi[3]
[1]*Department of Physics, National Taiwan University, Taipei, Taiwan, Republic of China*
[2]*Institute of Physics, Academia Sinica, Nankang, Taipei, Taiwan 11529, Republic of China*
[3]*Department of Polymer Science and Engineering, Inha University, Inchon, 402-751, Korea*
(Received 29 February 1996)

The thickness profiles of the aureole created in the bursting of vertical soap films are studied by a fast line scan charge-coupled device camera. Detail dynamics of the aureole are reported. Phenomena of the wavelike motions of the bursting rim and detachments of the aureole from the bursting film are also observed. We find that the stability of the aureole increases with the surfactant concentrations and is sensitive to the types of surfactant being used. The concentration dependence suggests that the interaction of micelles might be important in the bursting process. Furthermore, the surfactant monolayer in the aureole is found to be highly compressed and behaves like a rigid film. Existing theories of the aureole formation cannot account for all the observed phenomena. [S1063-651X(96)50810-X]

PACS number(s): 68.15.+e, 47.20.Dr, 47.40.−x

Two important findings in the studies of burstings of soap films [1–5] are the constant bursting velocity for a uniform film and the formation of an aureole ahead of the bursting front [4]. Interestingly, the bursting velocity $v_B=(\phi\sigma/\rho\delta)^{1/2}$ was obtained without any hydrodynamic considerations (also known as Culick's [2] velocity when $\phi=2$ [6]) where σ, ρ, and δ are the surface tension, density, and thickness of the soap film, respectively. In a shock wave model [7], the aureole is considered the shock front created by the surface tension gradient which is generated at the bursting rim by the fast compression of the surfactant molecules after bursting. Intuitively, both v_B and the shock velocity v_S should be determined by the physical properties of the bursting film through the interaction of the surfactant with the hydrodynamics of the burstings. However, as the behaviors of surfactants at the bursting rim are not well understood yet, one cannot obtain v_S from the shock wave theory without making some assumptions about the state of the surfactants and the form of v_B [7]. Therefore, detail comparisons of these theories with experiments are essential in the understanding of interactions of the surfactants at the bursting rim and its coupling to the bursting hydrodynamics.

Although experiments on burstings were started long ago [3,4,8], details of the formation of the aureole are still lacking. In this paper, we report results on the studies of burstings with a line scan charge-coupled device (CCD) camera that enables us to measure the thickness profiles during the burstings. The time dependence of the shape and velocity of the aureole is obtained for the first time. We found that the surfactant monolayer in the aureole is highly compressed and behaves like a rigid film. New phenomena of the wavelike motions of the bursting rim and detachments of the aureole from the bursting film are also observed. Existing theories cannot account for all the observed phenomena.

The setup of the experiment is similar to that of Ref. [4]. A vertical film of size 55 mm (height)×40 mm is formed by pulling a frame made of Plexiglas vertically out of a soap solution. Three nylon threads ($\sim\mu$m) are tied to the frame to form a rectangular boundary (the fourth side being the liquid-air interface) inside which the film will be formed. The soap solution is made by dissolving surfactants in a mixture of water and glycerin (63 wt % water, 37 wt % glycerin) [4]. Two systems of surfactants are used, namely, sodium dodecyl sulfate (SDS) and household detergent (MDW) (see Ref. [9]). The concentrations c of the samples are measured in units of the corresponding critical micelle concentrations (CMC) [10]. After the film is formed, a CCD camera is used to monitor the decreasing thickness of the film due to draining by measuring the positions of interference fringes formed from the reflection of a white light source. A white light laser (wavelength = 647, 568, 488 nm) is then used to calibrate the thickness at one spatial point by measuring the relative reflectance at these wavelengths. When the desired thickness is reached, the film is punctured by an electric spark [4]. A line scan CCD camera, 20 kHz line rate, is triggered to scan the film and record the bursting process. Therefore only one particular vertical or horizontal line, which is chosen to divide the film into two halves, on the film is being recorded. Experiments are performed in a temperature controlled room at 20 °C and the film is protected from the air motion.

Bursting images of SDS films are shown in Fig. 1. In Fig.1(a), with horizontal scanning, time is running downward and the reflected light from the film is shown as gray horizontal scan lines. A bright spot (spark) in Fig. 1(a) occurred near the middle of the film and initiated the bursting. For a time after the spark, the scan lines contain an increasing portion of a dark area, which is due to the loss of reflected intensity because of the bursting. Thus, the boundaries between the gray and dark regions in Fig. 1(a) define the trajectory of the bursting rim in the horizontal direction. From Fig. 1(a), it can be seen that the locus is on average a straight line but the boundary is not sharp. One can obtain from Fig. 1(a) an average v_B of 5.9 m/sec which is consistent with the measured δ of 1.8 μm with $\phi=1.9$.

Vertical scanning images of burstings are shown in Fig. 1(b) with 1.4 CMC SDS (inset) and 18 CMC SDS samples.

*Electronic address: PHCKCHAN@CCVAX.SINICA.EDU.TW

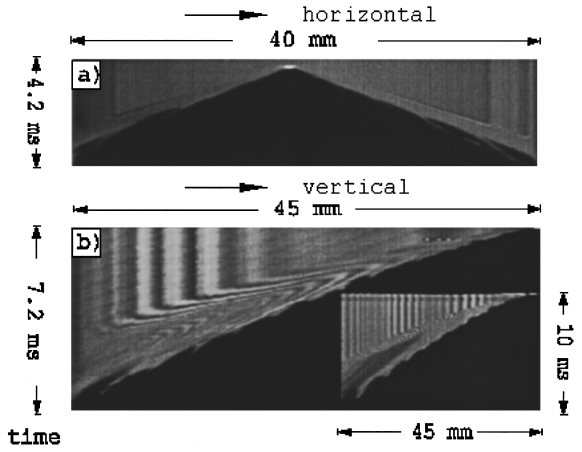

FIG. 1. Space-time images of the bursting process of a SDS vertical film taken by a line scan CCD. (a) 1.4 CMC sample, horizontal scanning with bursting at the middle and (b) 18 CMC sample, vertical scanning with bursting at the top. Concentration of the sample in the inset is 1.4 CMC. Angle between light source and camera is 60°.

Note that the horizontal axis of Fig. 1(b) is now the vertical direction and the bursting is initiated at the top. In Fig. 1(b), undisturbed films are marked by parallel vertical stripes (interference fringes due to nonuniform thickness). Three features are immediately visible in Fig. 1(b): (a) there is a wavelike motion of an unclear bursting rim, (b) there are detachments of the bursting front from the film (inset) and (c) a front which marks an abrupt change in thickness (twisting of the originally parallel vertical stripes) is running ahead

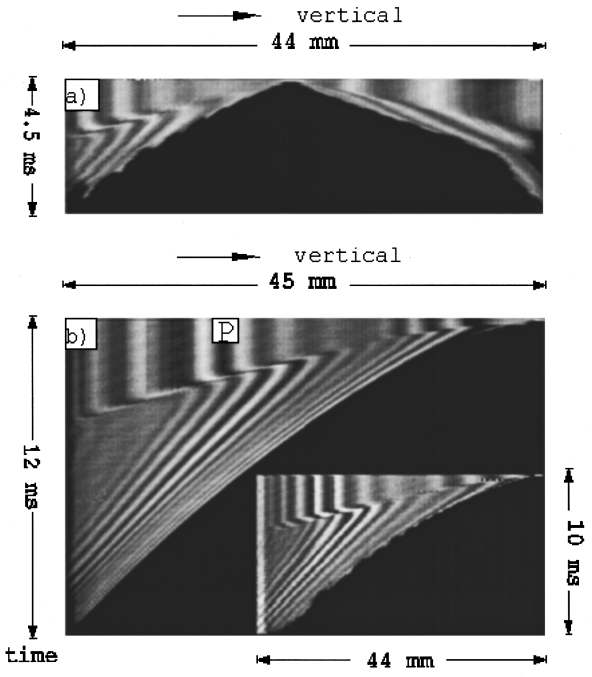

FIG. 2. Space-time images of the bursting process of a MDW vertical film taken by a line scan CCD with vertical scanning of a 120 CMC film (a) bursting at the middle and (b) bursting at the top. Concentration of the inset sample is 1 CMC. Angle between light source and camera is 60°.

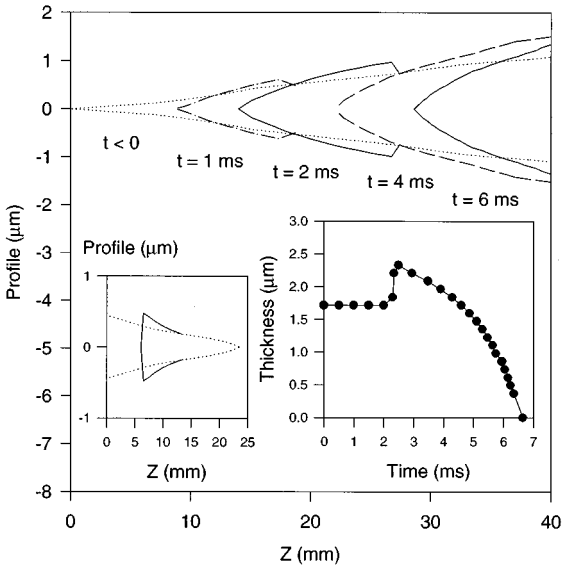

FIG. 3. Thickness profiles of the bursting film shown in Fig. 2(b) at various times after bursting ($t=0$). Uncertainties in the thickness are 0.25 μm. The right inset shows the thickness variations at a fixed point [point P in Fig. 2(b)] on the film. The left inset shows the upward moving aureole profile of Fig. 2(a) at 1 msec after bursting. Dotted lines are the profiles before bursting and Z is the distance in the vertical direction.

of the bursting rim. The structures in between the undisturbed film and the bursting rim are referred to as the aureole [4].

Various methods are tried to produce a more stable and clear aureole for quantitative studies. We found that the effective ways are the increase in c and the change to a suitable surfactant system. The unclear bursting aureole and detachment shown in the inset of Fig. 1(b) can be made to become more stable as shown in Fig. 1(b) by increasing the concentration of SDS from 1.4 CMC to 18 CMC [11]. However, when we change the surfactant to a household detergent (MDW), drastic effects are seen. Figure 2 shows the typical images of the vertical scanning of the bursting of MDW films which give more clear aureole. In Fig. 2(a), the film is punctured at the middle. It can be seen from the figure that the structures of the aureole are different for the downward and upward moving aureole. The thickness profile of the upward moving aureole, 1 msec after bursting, is shown in the left inset of Fig. 3. For the upward moving, no abrupt change of thickness is observed ahead of the bursting rim, similar to the findings of the Ref. [8]. However, for the downward bursting aureole, the interference fringes are twisted. To study the downward moving front more closely, we have performed experiments of bursting of vertical MDW films at the top for different concentrations shown in Fig. 2(b) and its inset. Similar to the results of SDS films, the aureole in the 1 CMC film (inset) is not as stable and clear as the 120 CMC film [(Fig. 2(b)]. One can also see that, except for a more stable aureole, the change of nearly 100 times in concentration does not seem to change the bursting dynamics much.

Figure 3 shows the thickness profiles obtained from Fig. 2. One clearly sees that the front of the aureole is the thickening of the film running ahead of the bursting rim. The right

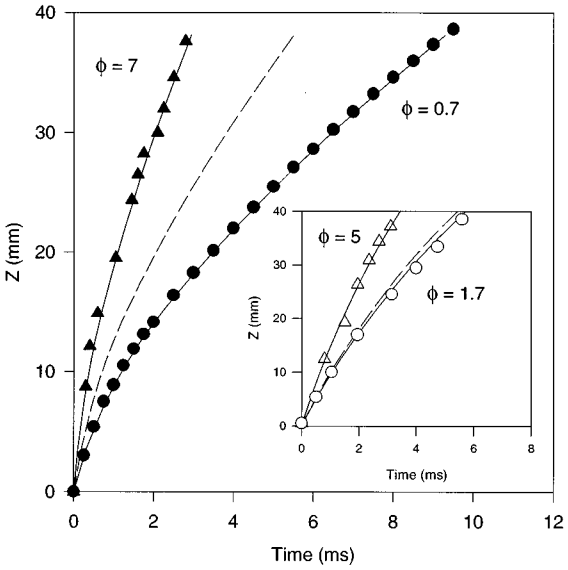

FIG. 4. Trajectories of the thickening front (filled triangles) and the bursting rim (filled circles) for 120 CMC MDW (inset, 18 CMC SDS). Solid lines are fits to v_B with ϕ shown next to the lines and broken lines are the trajectories of the Culick velocity with $\phi=2$. Uncertainties are smaller that the size of the symbols.

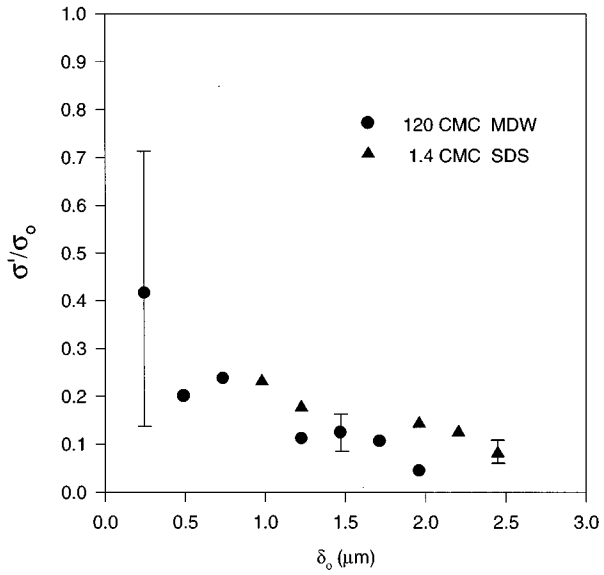

FIG. 5. Estimated surface tension in the aureole in the 120 CMC MDW and 1.4 CMC SDS samples as a function of thickness.

inset of Fig. 3 shows the abrupt increase in thickness of the point P in Fig. 2 when the bursting front arrives. This abrupt change of thickness is predicted by the shock wave model of Frankel and Mysels [7]. If one compares closely the interference patterns in Fig. 1(b) with those in Fig. 2(b), it can be seen that the changes in the thickness of the aureole of Fig. 1(b) are smooth compared with that of Fig. 2(b) and therefore the signature of a shock front is not as clear in the SDS film. Note also that the profiles of the film in Fig. 3 became monotonic 4 msec after the bursting because the thickening front already touched the boundary at this time and no undisturbed film was left.

We have calculated the rim velocity and checked for its thickness dependence for the experiments shown in Figs. 1(b) and 2(b). However, it is apparent from Fig. 3 that it is difficult to define a thickness for the bursting rim. Since the undisturbed film thickness is always used in earlier literature, we have plotted, in Fig. 4, the trajectories of the thickening front and bursting rim together with the trajectories given by $v_B=(\phi\sigma/\rho\delta)^{1/2}$ using the undisturbed film thickness and an adjustable ϕ for both the 18 CMC SDS and 120 CMC MDW samples. Note that the data do not fall on straight lines because the thickness of the undisturbed film is changing with position. The inset of Fig. 4 shows that the v_B of the SDS film can be fitted to $\phi_{rim}=1.7$ and the aureole front gives a value of $\phi_{au}=5$. The physical meaning of these values of ϕ is not clear yet. They are used here mainly for the convenience in comparison with earlier works and discussions of the two velocities. These two velocities give a ratio of $\gamma=(\phi_{au}/\phi_{rim})^{1/2}=1.7$ which is similar to the findings of [4]. However, for the bursting of MDW as shown in Fig. 4, we have $\phi_{rim}=0.7$ and $\phi_{au}=7$ which gives $\gamma=3.1$. Since a smaller ϕ_{rim} means that a smaller amount of energy is available for the bursting rim, it seems likely that more energy is dissipated in the sharper aureole of the MDW film.

Theoretically [7], the change in thickness $(\delta'-\delta_0)$ across the shock front is related to the surface tension changes $(\sigma'-\sigma_0)$ by $(u_s/u_c)^2[(\delta'-\delta_0)/\delta']=(\sigma_0-\sigma')/\sigma_0$, where u_s is the shock velocity and u_c the Culick velocity. Also, δ_0 and σ_0 are the thickness and surface tension of the undisturbed film respectively while δ' and σ' are those in the thickened film (aureole). This expression is used to estimate the changes in surface tension during burstings by using the changes in thickness as shown in the inset of Fig. 3 as $\delta'-\delta_0$ and (u_s/u_c) from Fig. 4. Results of the σ'/σ_0 at different film thickness during bursting for the 120 CMC MDW and 1.4 CMC SDS samples are shown in Fig. 5. In Fig 5, σ'/σ_0 decreases with increasing δ_0 and can get as low as 0.1. In fact, if we have used the results from the 18 CMC SDS sample, σ'/σ_0 can even be negative [4]. Note that $\sigma_s=\sigma_w-\sigma_0$ is the spreading pressure [12] of the surfactant monolayer where σ_w is the surface tension of water. The decrease of σ_0 in the undisturbed film to σ' in the aureole suggests that there is an increase in the compression of the surfactant monolayer. Presumably, small and even negative values of σ'/σ_0 come from the situation where σ_s is increased under a strong compression.

An interesting consequence of this strong compression is that the film can become rigid. It can be seen in Fig. 2(b) and Fig. 3 that, sometime after the bursting, when the shock front touches the boundary and no more undisturbed film is left, the shapes of the profiles of the bursting film at this stage ($t>4$ msec) change very little with time, suggesting the motion of a rigid film. This compression is limited to the region bounded by the rim and the shock front. One can define the compression ratio $\beta=A_{au}/(A_{au}-A_{rim})$, where A_{au} and A_{rim} are the area of the circles bounded by the shock front and the rim, respectively. It can be shown that $\beta=\gamma^2/(\gamma^2-1)$ and we get β_{SDS} and $\beta_{\mathrm{MDW}}=1.5$ and 1.1, respectively, for the cases shown in Fig. 4. The smaller compressibility of MDW films is consistent with the above rigid film findings and perhaps also the origin of a more stable aureole.

From the above discussions, it is clear that shock wave is clearly produced during the burstings. However, the details

of this shock production are system dependent. It is not clear why the more complex sample of MDW would generate better shock wave, clear aureole, and a smaller ϕ_{rim}. The detachment of the aureole and the wavelike motions of the rim seen in low concentration samples are presumably the results of hydrodynamic instabilities [12] induced by the motion of the aureole. It will be interesting to know whether the stabilizing effects produced by the increase in surfactant concentrations are related to the interaction of the closely spaced micelles [13] in the concentrated samples. The motion of the rigid film in the aureole might also be studied by methods similar to the bursting of a polymer film [14] where viscosity and elasticity are important.

The authors would like to thank Y. Y. Chen, Y. Couder, and Chi Yuan for useful discussions and C. Y. Chang of Kao Corp. (Taiwan) for providing useful information about the MDW sample. This work is supported mainly by the National Science Council of the ROC under Grant No. NSC-85-2112-M-001-038 and partly by C&L Softech.

[1] A. Dupré, Ann. Chim. Phys. **4**, 11 (1867); **4**, 194 (1867).
[2] F. E. C. Culick, J. Appl. Phys. **31**, 1128 (1960).
[3] I. Liebman, J. Corry, and H. E. Perlee, Science **161**, 373 (1968).
[4] W. R. McEntee and K. J. Mysels, J. Phys. Chem. **73**, 3018 (1969).
[5] J. F. Joanny and P. G. de Gennes, Physica A **147**, 238 (1987).
[6] ϕ is a numeric factor which is used to match experimental data. However, a larger ϕ means that more energy is available for the bursting rim and less energy is being dissipated. For details, see Ref. [4].
[7] S. P. Frankel and K. J. Mysels, J. Phys. Chem. **73**, 3028 (1969).
[8] A. T. Florence and G. Frens, J. Phys. Chem. **76**, 3024 (1972).
[9] Moore Dish Wash detergent from Kao (Taiwan) Co., is mainly composed of three different components with alkyl dimethyl amine oxide (nonionic), alkyl polyglucoside (nonionic), and sodium polyoxyethylene alkylsulfate (anionic/nonionic). The surface tension at 1 CMC is 25.43 dyn/cm at 20 °C.
[10] The CMC of SDS is taken as 8.3×10^{-3} M and we have measured the CMC of MDW as 0.5 cc in 1000 cc of solution, starting from which the surface tension is nearly constant with increase in surfactant concentration.
[11] The concentration 1.4 CMC is the same as Ref. [4]. The solution at 18 CMC is already unstable. Precipitation occurs if the solution is left unstirred for more than a few hours. Experiments were conducted when there was no precipitation.
[12] Y. Couder, J. M. Chomaz, and M. Rabaud, Physica D **37**, 384 (1989).
[13] O. Krichevsky and J. Stavans, Phys. Rev. Lett. **74**, 2752 (1995).
[14] G. DeBrégeas, P. Martin, and F. Brochard-Wyart, Phys. Rev. Lett. **75**, 3886 (1995).